

Analytical and experimental investigation into the resistance of vertical plug flow with coarse particles

Liu, Xiangwei; Yang, Shuhao; Pang, Yusong

DOI

[10.1016/j.oceaneng.2024.118253](https://doi.org/10.1016/j.oceaneng.2024.118253)

Publication date

2024

Document Version

Final published version

Published in

Ocean Engineering

Citation (APA)

Liu, X., Yang, S., & Pang, Y. (2024). Analytical and experimental investigation into the resistance of vertical plug flow with coarse particles. *Ocean Engineering*, 308, Article 118253.
<https://doi.org/10.1016/j.oceaneng.2024.118253>

Important note

To cite this publication, please use the final published version (if applicable).
Please check the document version above.

Copyright

Other than for strictly personal use, it is not permitted to download, forward or distribute the text or part of it, without the consent of the author(s) and/or copyright holder(s), unless the work is under an open content license such as Creative Commons.

Takedown policy

Please contact us and provide details if you believe this document breaches copyrights.
We will remove access to the work immediately and investigate your claim.

Green Open Access added to TU Delft Institutional Repository

'You share, we take care!' - Taverne project

<https://www.openaccess.nl/en/you-share-we-take-care>

Otherwise as indicated in the copyright section: the publisher is the copyright holder of this work and the author uses the Dutch legislation to make this work public.



Research paper

Analytical and experimental investigation into the resistance of vertical plug flow with coarse particles

Xiangwei Liu^{a,*}, Shuhao Yang^a, Yusong Pang^b

^a Logistics Engineering College, Shanghai Maritime University, No. 1550 Haigang Road, Shanghai, 201306, China

^b Section Transport Engineering and Logistics, Department Maritime and Transport Technology, Faculty Mechanical Engineering, Delft University of Technology, Mekelweg 2, 2628, CD Delft, the Netherlands

ARTICLE INFO

Keywords:

Plug flow
Deep-sea mining
Vertical lifting
Bulk solids
Two-phase flow

ABSTRACT

Deep-sea mining activities have lately attracted growing interest. Recent research has led to the development of a hydraulic–mechanical hybrid vertical lifting system for deep-sea mining. Predicting the resistance of vertical plug flow in this system is critical for its engineering design. In this paper, an analytical model was developed to determine the resistance of vertical plug flow in a hydraulic–mechanical hybrid vertical lifting system in the presence of coarse particles. A recent model of the stress transmission ratio for pneumatic plug flow was verified and applied to the proposed model of resistance. In addition, it is considered that the co-existence of turbulent and laminar flows in the fluid flowing through the particles provides the necessary pressure gradient. A test setup was built to measure the resistance of vertical plug flow with/without water, along with varying particle diameters, plug lengths, and lifting speeds. Comparisons between the predictions of the analytical model and experimental measurements showed that they deviated by less than 13.6% on average. This shows that the proposed analytical model can be used to predict the resistance of vertical plug flow involving coarse particles.

1. Introduction

The depletion of mineral resources in the ground poses a significant challenge to global economic development (Alhaddad et al., 2023; Sharma, 2022), while mineral resources found on deep seabed can supplement the supply of critical metals. Twenty-one billion tons of reservoirs of critical metals, including cobalt, nickel, and platinum, are estimated to be available on the deep seabed around the world (Wu et al., 2022). This has led to a significant growth in interest in deep-sea mining in recent years (Hein et al., 2013).

A typical deep-sea mining system consists of multiple collectors, a vertical lifting system, a production service vessel, and minerals transport vessels. Reviews of the status as well as trends of development of technologies and equipment for deep-sea mining are available in the literature (Wu et al., 2022; Ma et al., 2022; Kang and Liu, 2021). Hydraulic and pneumatic lifting systems are currently considered to be the most viable commercial systems for the vertical lifting of deep-sea minerals (Kang and Liu, 2021). Current hydraulic vertical lifting systems involve the flow of small particles with a low concentration of solids. It remains challenging for these systems to meet the required lifting capacity for commercial plans for deep-sea mining (Sharma,

2022).

A hydraulic–mechanical hybrid vertical lifting (HMHVL) system was recently proposed (Liu and Yang, 2024). Its working principle is shown in Fig. 1. Numerous carriers are driven by mechanical power to lift coarse particles upward in plug flow pattern in a vertical pipe. The tailings are transported downward in a parallel pipe. The two pipes are connected to each other so that the carriers can move freely from one to the other. Meanwhile, rotary jet pumps provide the pressure gradient required to enable the slurry to flow upward. The HMHVL system has the advantages of a high energy efficiency and a large throughput in terms of the particle size. Another benefit is that it can avoid crushing on the seabed.

A sound understanding of the mechanism of resistance is critical for the engineering design of the HMHVL system. It is evident from its working principle that it involves different flow patterns of solid–liquid flow. Such factors as the particle diameter and the concentration of solids can significantly influence the pattern of flow (Bartosik, 2020). We consider four patterns of flow in this study according to the particle size and the concentration of solids. The first is the flow of small particles with a low solid concentration, which can be simplified as single-phase flow. Several classic prediction models of the pressure drop for this

* Corresponding author.

E-mail address: xwliu@shmtu.edu.cn (X. Liu).

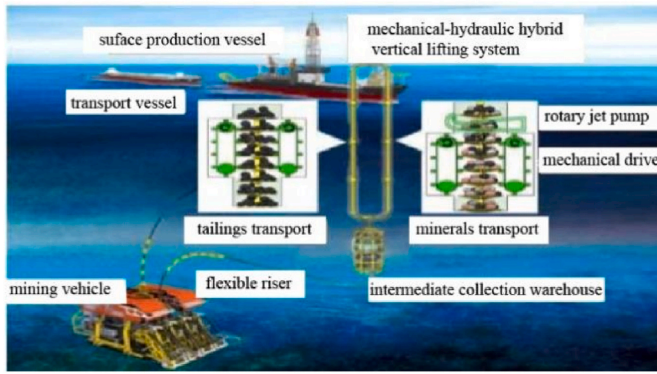


Fig. 1. Schematic overview of the proposed HMHVL system (modified from Fig. 1 in reference (Lee et al., 2015)).

pattern of flow have been developed (e.g., Durand, 1953; Newitt, 1955; Wilson, 1965). The distribution of particles in a pipe was considered in a model developed by Wasp et al. (1977). Past studies have also shown that the position of particles is mainly dependent on their Reynolds number (Feng and Michaelides, 2003). The effect of the shape of the particles on their settling behavior has also been investigated through numerical experiments, and the results have shown that the settling velocity of rectangular particles is lower than that of elliptical particles (Yokojima et al., 2021).

The second pattern of flow is that of coarse particles with a low solid concentration. Particle–fluid interactions become important in this pattern of flow. Engelmann developed empirical models for this pattern of flow, involving particles with diameters of 13–52 mm (Engelmann, 1978). Xia (2002) studied the energy loss due to particle–particle collision, and established a model for the total pressure drop in pressure for this pattern of flow. Matousek (2009) studied the vertical flow of three kinds of granular slurries. His results showed that particle–fluid interaction was the main cause of the pressure drop. Chung et al. (1998) conducted hydraulic lifting experiments using vertical pipes to identify the relationship between the solid concentration and the characteristics of flow. Measurements of concentration are especially challenging for this pattern of flow. Van Wijk et al. (2022) proposed a method of measurement by using a conductivity concentration meter. Li et al. (2018) examined the interactions between particles of different sizes and the slurry, and used the results to propose a model to calculate the pressure drop of flow involving particles of multiple sizes in high-concentration slurry based on the distribution of particle size and the velocity of flow. Li et al. (2020) investigated the addition of fine particles to a slurry of coarse particles in a pipeline. The results showed that adding fine particles considerably reduced the resistance in the pipeline by changing the regime of flow of coarse particles near the critical velocity of flow.

The third pattern of flow is that of small particles with a high solid concentration. The energy loss due to friction between particles, and that between particles and the pipe wall are dominant in this pattern of flow. The pneumatic lifting of small particles with a high solid concentration—namely, dense phase flow or plug flow—has been investigated in greater depth than their hydraulic lifting. Konrad (1980) developed a model to calculate the pressure drop of plug flow that has been widely accepted and used. The Konrad model considers the passive and active stress states of the particles within a plug, which leads to predictions of the upper and lower bounds of the pressure drop. The results of experiments have shown that the measured pressure drop of plug flow is somewhere between the upper and lower bounds of the Konrad model (Konrad and Totah, 1989). Niederreiter and Sommer developed a test device to measure the normal stress and that induced by the friction of the pipe wall when a plug passed through it (Niederreiter and Sommer, 2004). Their measurements confirmed that the ratio of stress transmission between axial stress and radial stress was somewhere between

the upper and lower bounds. Shaul and Kalman claimed that only the drag force of the pressure drop should be considered in the force balance of a plug slice (Shaul and Kalman, 2014). Based on this idea, they developed models of resistance for both horizontal and vertical pneumatic plug flows. A unique test setup was subsequently developed to measure the pressure drop and frictional forces in horizontal and vertical plug flows (Rabinovich et al., 2012). Rabinovich et al. used the results of their experiments to develop a model for the ratio of stress transmission, and found that its value was exponential with respect to the ratio between the plug length and the pipe diameter. Yang et al. analyzed the plugs used in vertical pneumatic lifting, and found that an active ratio of stress transmission was suitable for predicting the drop in pressure in case of the vertical pneumatic conveying (Yang et al., 2020).

The final pattern of flow is that of coarse particles with a high solid concentration. Scant research has been conducted on this pattern of flow thus far (Bartosik, 2020; Messa and Malavasi, 2013; Miedema, 2017). The particle–wall interaction becomes dominant in this case, and leads to a much higher friction of the wall compared with that in single-phase flow. Models of the pressure drop have been developed to predict the resistance under this pattern of flow (Shook and Bartosik, 1994). van Wijk developed a two-layer model of plug resistance (van Wijk et al., 2014) in which the flow of fluid flowing through a plug was assumed to be laminar, and the pressure gradient was calculated by using the Darcy equation. In addition, coarse particles within a plug were assumed to be in a state of active stress in the van Wijk model. The model predicted that the particle–wall friction increased exponentially with the plug length. However, it neglected the inertia of the fluid. The above analysis shows that a limited amount of research has been conducted on the vertical plug flow of coarse particles, because of which predicting the resistance of this kind of flow remains a challenge in both research and practice.

This study develops an analytical model to determine the resistance of vertical plug flow. In Section 2, we describe the development of the proposed model. Section 3 introduces an experimental investigation into the measurement of resistance during vertical lifting. We compare the results of the analytical model with those of experimental measurements and discuss their implications in Section 4. The conclusions of this study are summarized in Section 5.

2. Development of the resistance model

Firstly, the forces acting on a vertical plug during lifting is analyzed. As is shown in Fig. 2, a plug may be subjected to five forces during

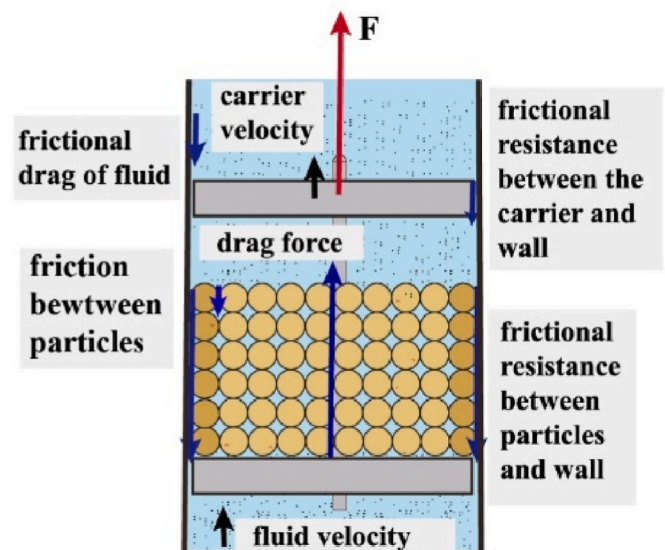


Fig. 2. Schematic of forces acting on a vertical plug during lifting.

operation: the friction between particles, friction between particles and the pipe wall, friction between the carrier and the pipe wall, drag force of the fluid flowing through the plug, and the frictional drag of the fluid due to the pipe wall. The developed model of the resistance of vertical plug flow needs to take all these forces into account.

To determine the friction between the particles and the pipe wall, one need to calculate the normal stress exerted on the latter when a plug passes through it. From the analysis of a differential slice of the particle plug, we have the following equation of force balance:

$$dF_g + dF_{p-w} = dF_p + dF_d + dF_b \quad (1)$$

in which F_g refers to the gravity of particles in air (N), F_b refers to the buoyant force experienced by the particles (N), F_p refers to the compression force on the plug slice by the particles above the slice (N), F_{p-w} refers to the frictional resistance between the particles and the pipe wall (N), and F_d refers to the drag force from the fluid flowing through the particle plug (N).

Fig. 3 shows the stresses acting on a differential slice of the plug. Pressure acts on both the top and bottom of the slice in addition to the buoyancy of the fluid, the gravity of the particles, and the wall friction.

Given the formulae for calculating the gravity of the particles, buoyancy, and frictional resistance, Eq. (1) can be rewritten as:

$$A\rho_b(1-\varepsilon)gdz + \tau_w\pi Ddz = d\sigma_z A + A\frac{\Delta P}{L}dz + A\rho_f(1-\varepsilon)gdz \quad (2)$$

where A refers to the area of cross-section of the pipe (m^2), σ_z refers to the pressure on top of the slice (MPa), τ_w refers to the frictional stress between the particles and the pipe wall (MPa), D refers to the pipe diameter (m), L refers to the length of the slice (m), ε refers to the porosity, ρ_b refers to the density of the particles (kg/m^3), ρ_f refers to the density of the fluid (kg/m^3), and ΔP refers to the pressure drop of the fluid flowing through the differential slice (MPa).

The frictional stress between the particles and the pipe wall can be calculated as:

$$\tau_w = \mu_w \sigma_x \quad (3)$$

where μ_w denotes the coefficient of friction between the particles and the pipe wall, σ_x refers to the normal pressure on the pipe wall exerted by the particles (MPa).

There is a complex relationship between the axial and radial stresses within a particle plug. The Janssen model is applied to obtain the radial stress (Sperl, 2006), and a coefficient of stress transmission is used to describe this relationship, which is:

$$\sigma_x = k\sigma_z \quad (4)$$

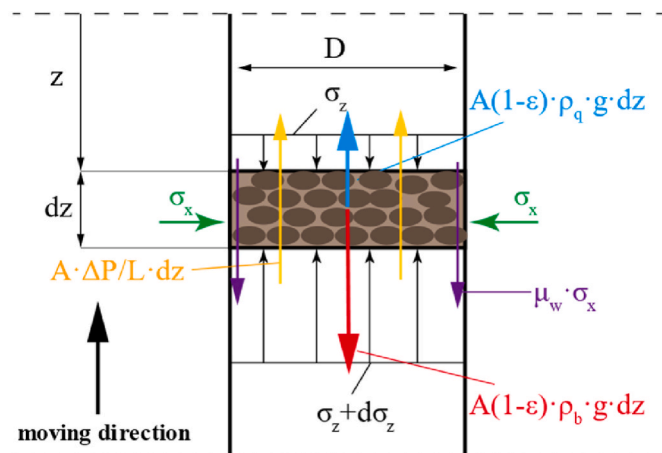


Fig. 3. Analysis of the stress of a plug slice.

in which k denotes the coefficient of stress transmission.

Equation (2) can then be rewritten as:

$$\frac{\pi D^2 d\sigma_z}{4} - \frac{\pi D^2 \rho_b(1-\varepsilon)gdz}{4} - \mu_w \pi D k \sigma_x dz + \frac{(\pi D^2) \Delta P}{4L} dz + \frac{\pi D^2 \rho_f(1-\varepsilon)gdz}{4} = 0 \quad (5)$$

Equation (5) can be simplified as:

$$d\sigma_z - \left[(\rho_b - \rho_f)(1-\varepsilon)g - \frac{\Delta P}{L} \right] dz - \mu_w \frac{4}{D} k \sigma_x dz = 0 \quad (6)$$

Equation (6) is a first-order linear differential equation for which an analytical solution is available. The pressure at the top of the plug is assumed to be as follows:

$$\sigma_z(z=0) = 0 \quad (7)$$

Therefore, the axial stress within a plug can be calculated as:

$$\sigma_z = \frac{\left((\rho_b - \rho_f)(1-\varepsilon)g - \frac{\Delta P}{L} \right) D}{4\mu_w k} \left(e^{\frac{4\mu_w k}{D} z} - 1 \right) \quad (8)$$

The frictional force between the particles and the wall can be calculated by integrating the friction-induced stress over the total height of the plug:

$$F_{p-w} = \int_0^h \pi \mu_w D \sigma_x dz = \frac{\pi \left((\rho_b - \rho_f)(1-\varepsilon)g - \frac{\Delta P}{L} \right) D^3}{16\mu_w k} \left(e^{\frac{4\mu_w k}{D} h} - 1 \right) - \frac{\pi \left((\rho_b - \rho_f)(1-\varepsilon)g - \frac{\Delta P}{L} \right) D^2 h}{4\mu_w k} \quad (9)$$

in which h is the height of the plug (m).

It is clear that the coefficient of stress transmission and the pressure drop need to be known in order to calculate the frictional force of the wall.

The velocity of the fluid is higher than that of the plugs in the HMHVL system. Fig. 4 depicts the fluid flowing through a vertical plug, which can be considered to be a particle-stacking bed.

Based on Bernoulli's equation, we have the following relationship between fluid flows at points 1 and 2:

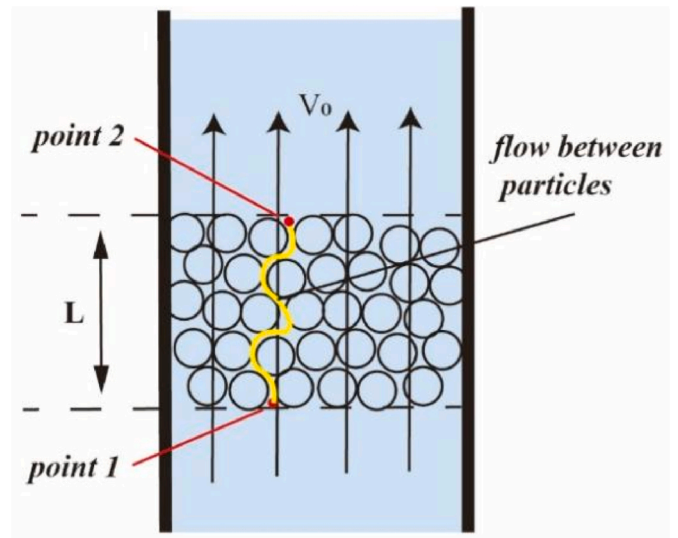


Fig. 4. Fluid flowing through particles in a plug.

$$\frac{p_1}{\rho_f} + gz_1 + \frac{\alpha_1 v_1^2}{2} - h_f = \frac{p_2}{\rho_f} + gz_2 + \frac{\alpha_2 v_2^2}{2} \quad (10)$$

where p denotes the pressure (MPa), z represents the height (m), α represents the coefficient of motion, v represents the velocity (m/s), h_f represents the loss of friction, and "1" and "2" refer to points 1 and 2, respectively.

As the plug is short, the change in the velocity of the fluid from point 1 to 2 can be neglected. One then has the following relationship:

$$\frac{\Delta p}{\rho_f} = h_f \quad (11)$$

It is clear from Equation (11) that the pressure drop of the fluid flowing through the plug is caused by the loss of friction. The latter can be calculated as the loss in the drag of the fluid passing through many small tubes (Coker, 2007):

$$h_f = 4C_f \frac{L_{pipe}}{D_{pipe}} \frac{\bar{v}^2}{2} \quad (12)$$

where C_f denotes the drag coefficient, \bar{v} denotes the mean velocity of the fluid (m/s), L_{pipe} denotes the equivalent pipe length (m), and D_{pipe} denotes the equivalent pipe diameter (m).

The fluid travels through the gaps between the particles. The equivalent pipe length is greater than the plug height, and is related to its tortuosity λ by the relation given by Bear (1972):

$$L_{pipe} = \lambda L \quad (13)$$

in which λ denotes the tortuosity of the flow path.

The tortuosity of the flow path is approximated by using research by Yu and Li (2004):

$$\lambda = \frac{1}{2} \left[1 + \frac{1}{2} \sqrt{1 - \varepsilon} + \sqrt{1 - \varepsilon} \frac{\sqrt{\left(\frac{1}{\sqrt{1 - \varepsilon}} - 1\right)}}{1 - \sqrt{1 - \varepsilon}} \right] \quad (14)$$

in which ε refers to porosity of the granular bed.

The equivalent pipe diameter can be expressed as (Wu et al., 2008):

$$D_{pipe} = \frac{2}{3} \frac{\varepsilon}{1 - \varepsilon} \varphi d_p \quad (15)$$

where φ denotes the sphericity of the particle, and d_p denotes the particle diameter (m).

In addition, following relationship exists between the velocity of the fluid in the particle plug and the velocity of the fluid flowing out of the plug:

$$\bar{v} = \frac{v_0}{\varepsilon} \quad (16)$$

where v_0 denotes the velocity of the fluid coming out of the plug (m/s) while \bar{v} denotes that of the fluid inside the plug (m/s).

When the flow regime of the fluid is laminar, the drag coefficient can be calculated as (Coker, 2007):

$$C_f = \frac{16}{Re} \quad (17)$$

When the flow regime of the fluid is turbulent, the following relationship holds:

$$3C_f \lambda = 1.75 \quad (18)$$

In case of the two-phase flow of particles with a small Reynolds number, the viscous effect of the fluid is primarily considered. In this case, the Blake–Kozeny equation can be applied to calculate the drop in pressure (Ergun, 1952):

$$\frac{\Delta p}{L} = \frac{150 v_0 \mu (1 - \varepsilon)^2}{\varepsilon^3 (\Phi d_p)^2} \quad (19)$$

In case of the two-phase flow of particles with a large Reynolds number, the inertia of the fluid should also be taken into account. In this case, the Burke–Plummer equation can be used to calculate the drop in pressure (Ergun, 1952):

$$\frac{\Delta p}{L} = \frac{1.75 \rho_f v_0^2 (1 - \varepsilon)}{\Phi d_p \varepsilon^3} \quad (20)$$

The Ergun equation predicts the pressure drop of a fluid flowing through a particle plug, and can be obtained by combining Equations (18) and (19) (Ergun, 1952):

$$\frac{\Delta p}{L} = \frac{150 v_0 \mu (1 - \varepsilon)^2}{\varepsilon^3 (\Phi d_p)^2} + \frac{1.75 \rho_f v_0^2 (1 - \varepsilon)}{\Phi d_p \varepsilon^3} \quad (21)$$

The pressure drop of a fluid flowing through a vertical plug for coarse particles is calculated in the model of resistance proposed in this study by applying the Ergun equation.

A mechanical lifting force is needed to transport the particles upward in the HMHVL system. Based on the analysis of forces acting on the plug, the mechanical lifting force can be calculated as:

$$F_t = F_{p-w} + F_g - F_b - F_d \quad (22)$$

where F_t refers to the mechanical lifting force for the plug (N).

By using Equations (9) and (21), one can obtain the mechanical lifting force required to lift a plug as:

$$F_t = \frac{\pi D^2}{4} \sigma_z = \frac{\pi \left((\rho_b - \rho_f) (1 - \varepsilon) g - \frac{\Delta p}{L} \right) D^3}{16 \mu_w k} \left(e^{\frac{4 \mu_w k}{D} z} - 1 \right) \quad (23)$$

3. Experimental study

A test setup for hydraulic–mechanical hybrid vertical lifting was developed to measure the mechanical lifting force for vertical plug flow with coarse particles (see Fig. 5). The setup consisted of a closed pipe loop, a centrifugal pump, an electromagnetic flowmeter (JIMTEC DN200), a water tank, a valve, a receiving tank, a motor, a wire equipped with a tension sensor (CHENGTEC CT1000), and a carrier. Water could circulate in the closed pipe loop, and its rate of flow was recorded by using the flowmeter. The vertical pipe was composed of transparent PVC, and had an inner diameter of 200 mm and a height of 4.5 m. The motor pulled the wire to provide a lifting force to the carrier, which was equal to resistance of vertical plug flow when its velocity was stable. The lifting force was recorded by the tension sensor.

To form a plug flow in the vertical pipe, a carrier was designed to hold coarse particles as the plug. Fig. 6 shows the components used to form the particle plug. Small holes were drilled into the two disks of the carrier to allow water to flow through it while preventing coarse particles from falling behind. The length of the carrier was 500 mm, and the maximum weight of the particles that it could hold was 15 kg.

With this test setup, we could investigate different experimental conditions to determine the contributions of different components to the resistance of vertical plug flow. We designed three experimental conditions.

- 1) Without water condition: There was no water in the vertical pipe. This condition was achieved by closing the valve in the test setup. Under this condition, the wire provided all the mechanical force required to lift the plug up inside the pipe. The force measured by the tension sensor consisted of the friction between the plug and the pipe wall, and the weight of the plug.

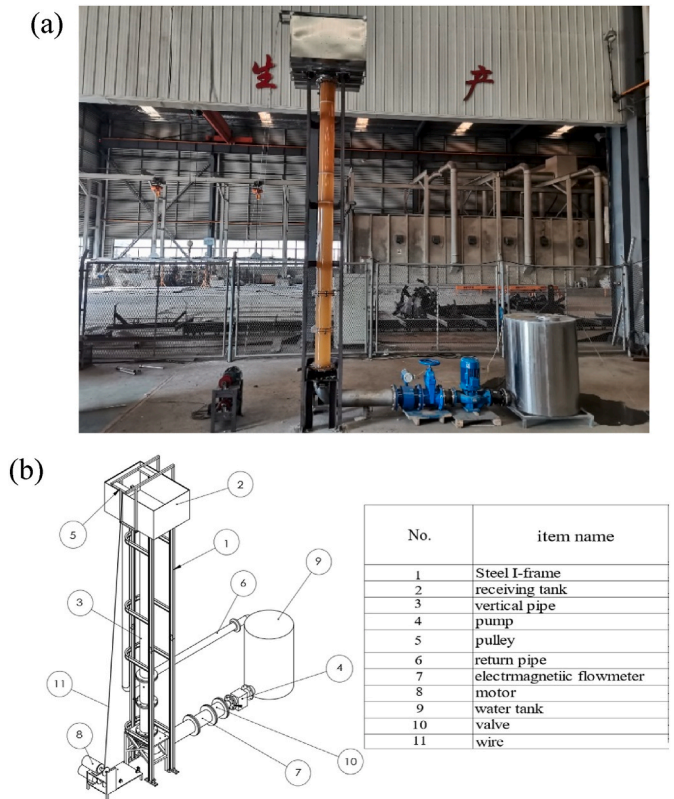


Fig. 5. Test setup. (a) photograph of the site; (b) items used in the test setup.

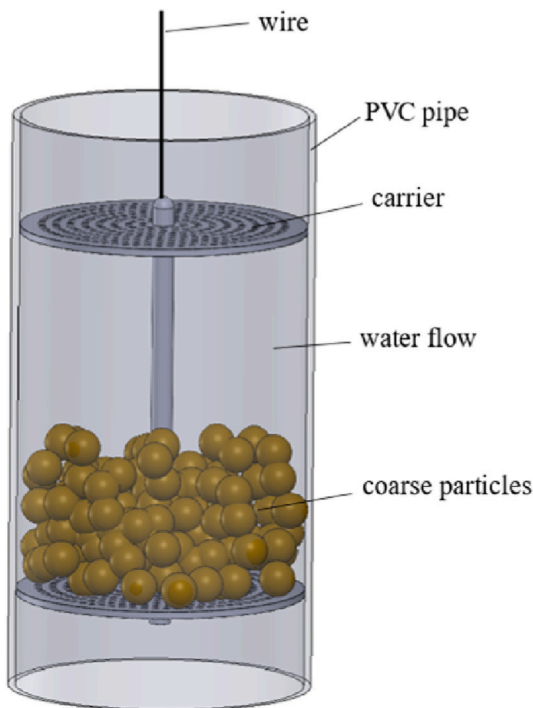


Fig. 6. Structure of the carrier.

2) Static water condition: Water was kept still in the pipe while the plug was lifted by the wire. This was achieved by first filling the vertical pipe with water and then closing the valve. The lifting force measured by the tension sensor consisted of the pressure drop of the

plug moving through static water, the friction between the plug and the wall, and the weight of the plug in the fluid.

3) Hydraulic auxiliary condition: Water flowed at the same velocity as that at which the plug moved upward. This was achieved by simultaneously controlling both the motor and the valve. The measured lifting force consisted of the pressure drop of water flowing through the plug, the friction between the plug and the pipe wall, and the weight of the plug in the fluid.

We used cobbles with diameters of 13, 18, and 25 mm as the coarse particles in the experiments (Fig. 7). The coefficient of friction between the cobbles and the wet PVC pipe was 0.301, and the coefficient of friction between the cobbles and the dry PVC pipe was 0.46, which were measured by using a test instrument (type: DHKFC-1).

The steps of the test were as follows. The particles were first screened and weighted, and were then used to fill the holding part of the carrier, which was lowered to the bottom of the vertical pipe. We used particles of different weights to obtain different length-to-diameter ratios of the plug. When the plug weighed in the range of 5–10 kg, the ratio of the plug length of the particle to the particle plug diameter r varied from 0.45 to 0.945 (see Fig. 8). Once the carrier had been appropriately placed, the valve, pump, and motor were turned on/off manually according to different experimental conditions. The speed of the carrier, lifting force of the wire, and rate of water flow were simultaneously recorded. Each test was repeated three times.

Table 1 lists all tests that were conducted in this study. A total of 36 groups of tests were carried out with different combinations of the lifting velocity, plug weight, and particle diameter along with other experimental conditions.



Fig. 7. Cobbles used in this experimental study.

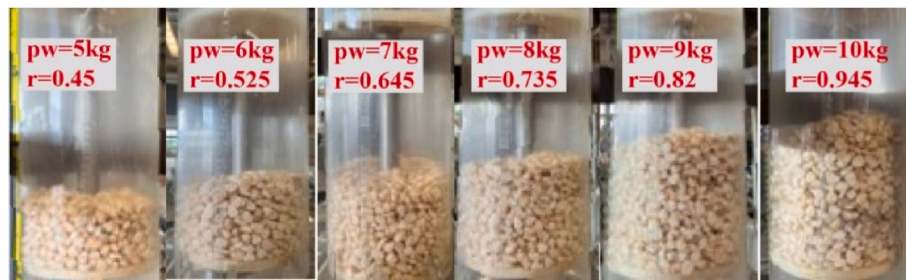


Fig. 8. Photographs of the coarse particles plugs in the tests. Note: "pw" refers to particle weight, and "r" refers to the ratio between plug length and diameter.

Table 1
Overview of the tests conducted in this study.

Test No.	Lifting velocity (m/s)	Particle diameter (mm)	Weight (kg)	Experimental condition
1	0.02	13	5,6,7,8,9,10	Without water
2	0.05	13	5,6,7,8,9,10	Without water
3	0.08	13	5,6,7,8,9,10	Without water
4	0.1	13	5,6,7,8,9,10	Without water
5	0.02	18	5,6,7,8,9,10	Without water
6	0.05	18	5,6,7,8,9,10	Without water
7	0.08	18	5,6,7,8,9,10	Without water
8	0.1	18	5,6,7,8,9,10	Without water
9	0.02	25	5,6,7,8,9,10	Without water
10	0.05	25	5,6,7,8,9,10	Without water
11	0.08	25	5,6,7,8,9,10	Without water
12	0.1	25	5,6,7,8,9,10	Without water
13	0.02	13	5,6,7,8,9,10	Static water
14	0.05	13	5,6,7,8,9,10	Static water
15	0.08	13	5,6,7,8,9,10	Static water
16	0.1	13	5,6,7,8,9,10	Static water
17	0.02	18	5,6,7,8,9,10	Static water
18	0.05	18	5,6,7,8,9,10	Static water
19	0.08	18	5,6,7,8,9,10	Static water
20	0.1	18	5,6,7,8,9,10	Static water
21	0.02	25	5,6,7,8,9,10	Static water
22	0.05	25	5,6,7,8,9,10	Static water
23	0.08	25	5,6,7,8,9,10	Static water
24	0.1	25	5,6,7,8,9,10	Static water
25	0.02	13	5,6,7,8,9,10	Hydraulic auxiliary
26	0.05	13	5,6,7,8,9,10	Hydraulic auxiliary
27	0.08	13	5,6,7,8,9,10	Hydraulic auxiliary
28	0.1	13	5,6,7,8,9,10	Hydraulic auxiliary
29	0.02	18	5,6,7,8,9,10	Hydraulic auxiliary
30	0.05	18	5,6,7,8,9,10	Hydraulic auxiliary
31	0.08	18	5,6,7,8,9,10	Hydraulic auxiliary
32	0.1	18	5,6,7,8,9,10	Hydraulic auxiliary
33	0.02	25	5,6,7,8,9,10	Hydraulic auxiliary
34	0.05	25	5,6,7,8,9,10	Hydraulic auxiliary
35	0.08	25	5,6,7,8,9,10	Hydraulic auxiliary
36	0.1	25	5,6,7,8,9,10	Hydraulic auxiliary

4. Results and discussion

Fig. 9 shows an example of the measurement of the raw lifting force by the tension sensor during the test with a plug weighing 7 kg, a lifting speed of 0.05 m/s, and particle size of 25 mm. Four processes could be distinguished during a given test: the stationary process ①, the lifting process ②, the stationary process after the lifting process ③, and the

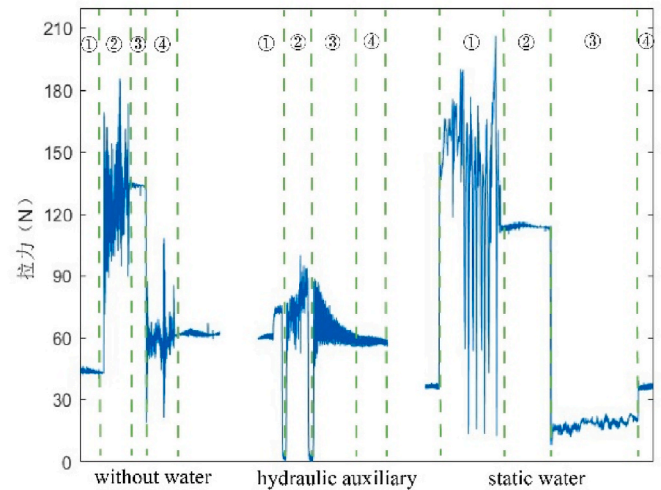


Fig. 9. Raw measurement data of the lifting force under three experimental conditions. Note: ① denotes the stationary process; ② denotes the lifting process; ③ denotes stationary after lifting process; ④ denote the descending process.

descending process ④. The stationary process revealed the tension on the particle plug before lifting, the lifting process showed the tension on the particle plug during lifting, the stationary process after the lifting process described the tension acting on the particles after lifting, while the descending process revealed the tension acting on the particles during descent. Because the control over these four processes were artificial, their timing was different between experiments. Fig. 9 also shows that the force required to keep the carrier stationary after it had descended to the bottom under the static water condition was the smallest of the three experimental conditions considered. This was due to the buoyant force. The force required to lift the carrier under the static water condition was the largest while that under the hydraulic auxiliary condition was the smallest. This is because the water acted as a resistance under the static water condition but as a driving force under the hydraulic auxiliary condition. In addition, we observed significant fluctuations in the measured force during the lifting process because the plug was subjected to the cyclic formation and breakage of force chains within the particles in the plug.

Fig. 10 shows the measured force required to lift the plug under the three experimental conditions in case of particles with a diameter of 25 mm. The measured force was calculated based on the mean value of the lifting forces in three repeated tests. In general, as the weight of the plug increased, a larger force was observed. Fig. 10(a) shows the lifting force under the hydraulic auxiliary condition. As the weight of the plug increased, there was a nearly linear increase in the measured force. Fig. 10(b) shows the lifting force in the absence of water. When the plug weighed between 5 and 10 kg, a gentle increase in the lifting force was observed. Divergence was observed because the plug vibrated during the tests when it weighed 8–9 kg and the lifting speed was 0.08 m/s. Fig. 10

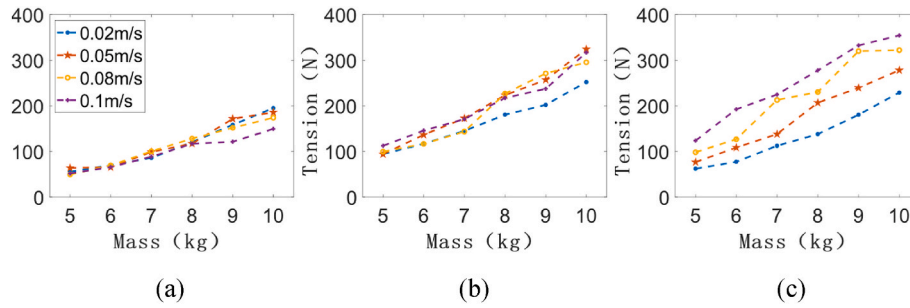


Fig. 10. Measured lifting forces with particles with a diameter of 25 mm. (a) hydraulic auxiliary condition, (b) without water, and (c) with static water.

(c) shows the lifting force under the static water condition. It is clear from it that the lifting force increased significantly with the plug weight and the lifting speed. In addition, a larger force was required under the static water condition compared with the other two experimental conditions.

Determining the coefficient of stress transmission is challenging. The upper and lower bounds of this coefficient are determined in the traditional method by applying the passive and active states of stress, respectively. Recently, Shaul and Kalman developed a model for the coefficient of stress transmission (Shaul and Kalman, 2014):

$$k = \frac{a\mu_e + f(\alpha)}{D} r^{-0.6} \quad (24)$$

in which μ_e denotes the coefficient of internal friction, r refers to the ratio of the plug length of particles to their plug diameter, α is a dimensionless constant, $f(\alpha)$ is a function of the inclination of the pipe, and D_{50} refers to a diameter of the pipe of 50 mm.

With transformation to Equation (23), the coefficient of stress transmission k can be expressed as:

$$k = \frac{D}{4\mu_w} \ln \left\{ \frac{16\mu_w F_t + \pi[(\rho_b - \rho_f)(1 - \varepsilon)g]}{\pi[(\rho_b - \rho_f)(1 - \varepsilon)g]} \right\} \quad (25)$$

in this case study the density of the particles is 2650 kg/m^3 , the density of the fluid is 1000 kg/m^3 , the porosity is 38%, the coefficient of friction between the particles and the wall is 0.46.

Equation (25) can be used to calculate the coefficient of stress transmission. For particles with sizes of 13 mm, 18 mm, and 25 mm in the lifting condition without water, with the measured lifting force F_t , we obtained the indirectly measured coefficient of stress transmission for each test (see Fig. 11).

Based on Shaul and Kalman's model, by applying curve fitting, one can obtain the coefficient of stress transmission as a function of the ratio r between the plug length and diameter with given plug conditions for three particle sizes 13 mm, 18 mm, and 25 mm: $k_{13} = 1.897r^{-0.56}$ (26)

$$k_{18} = 1.584r^{-0.56} \quad (27)$$

$$k_{25} = 1.052r^{-0.56} \quad (28)$$

Fig. 11 compares the indirectly measured coefficient of stress transmission in this study with the results based on Shaul and Kalman's model. The results of regression analysis show that Shaul and Kalman's model matched well with the measurements of the coefficient of stress transmission. We thus used Shaul and Kalman's model of the coefficient of stress transmission in our proposed model of resistance. The value of R^2 decreased with increasing particle size may be because Shaul and Kalman considered particles with a diameter smaller than 4 mm in their experiments while the particle size is much larger in current study.

In order to evaluate the performance of the developed model of resistance, the deviation between the predictions of the lifting force from

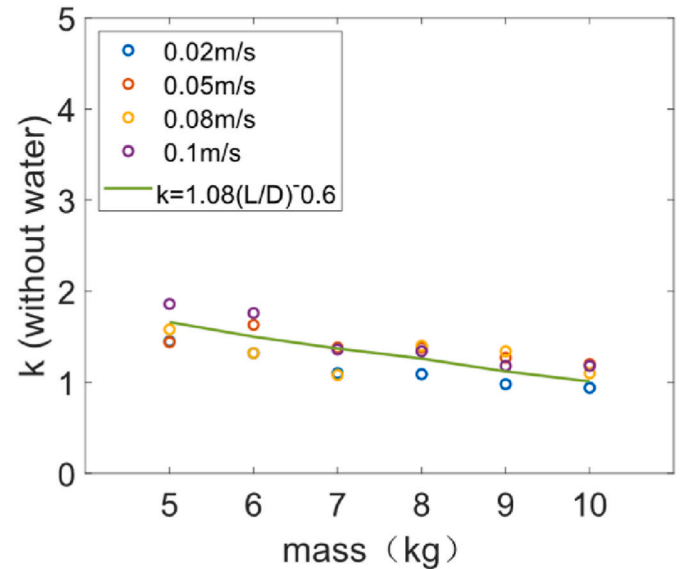


Fig. 11. Comparison between the measured and predicted ratios of stress transmission without water, with particles with sizes of (a) 13 mm, (b) 18 mm, and (c) 25 mm.

the developed model of resistance and the measured lifting force during the tests need to be calculated:

$$\delta = \frac{|F_{t,m} - F_{t,c}|}{F_{t,m}} \quad (29)$$

In the above, δ is the deviation between the experimentally measured and theoretically calculated lifting forces, $F_{t,m}$ refers to experimentally measured lifting force (N), and $F_{t,c}$ is the theoretically calculated lifting force from the model of resistance (N).

Fig. 12 shows the deviations between the experimental measurements and theoretical calculations for different tests. In general, the deviation between the theoretical predictions and the measured data was independent of the lifting speed and plug weight. The average deviation between them was 10.8% for particles with a diameter of 13 mm. A maximum deviation of 27% was observed when the lifting speed was 0.08 m/s and the plug weight was 7 kg. For particles with a diameter of 18 mm, the average deviation between the predictions of the proposed model and the experimental results under the three experimental conditions was 13.6%. The maximum deviation between them was 35% under the hydraulic auxiliary condition. The average deviation for particles with a diameter of 25 mm was 11.3%, while a maximum deviation of 28% was observed under the hydraulic auxiliary condition. It is evident from this that the predictions of the proposed model of resistance matched reasonably well with the experimental measurements. This verifies the accuracy of our proposed analytical model.

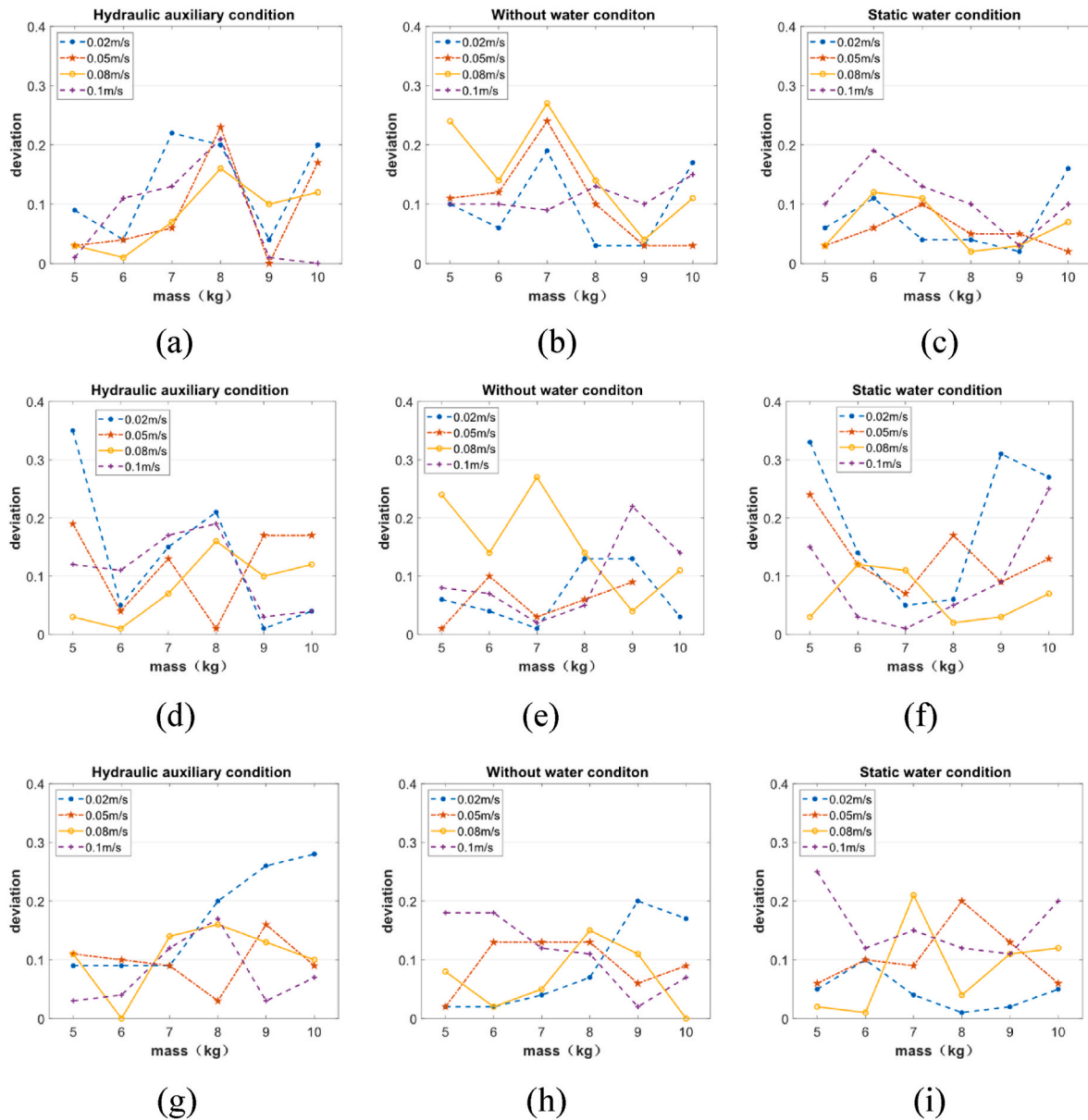


Fig. 12. Comparisons between the results of the proposed model of resistance and the experimental measurements. (a) $d_p = 13$ mm, hydraulic auxiliary condition; (b) $d_p = 13$ mm, without water; (c) $d_p = 13$ mm, static water condition; (d) $d_p = 18$ mm, hydraulic auxiliary condition; (e) $d_p = 18$ mm, without water; (f) $d_p = 18$ mm, static water condition; (g) $d_p = 25$ mm, hydraulic auxiliary condition; (h) $d_p = 25$ mm, without water; (i) $d_p = 25$ mm, static water condition.

We observed some randomness in the experimental measurements for three reasons. First, the particle diameters were somewhat random. Although the particles were sieved by using standard screens, some randomness in their distribution persisted. Second, the shape of the particles was random, and this impacted the measured lifting force during the tests. Third, the plug vibrated during the lifting process in some tests. This might have contributed to the deviation in the measurements.

5. Conclusions

In this paper, we proposed an analytical model of resistance during hybrid hydraulic–mechanical vertical plug flow with coarse particles. The model considers the coefficient of transmission between axial and radial stress. It also considers the inertia of the fluid by applying the Ergun equation to calculate the pressure drop. A test setup was developed to measure the forces required to lift vertical plugs with coarse particles with/without water. Comparisons between the theoretical

predictions of the model and the experimental measurements showed that the average deviation between them was smaller than 13.6%. Therefore, the proposed analytical model can be used to accurately predict the resistance of vertical plug flow with coarse particles. Due to the limitation of the test setup, however, the measurements of the lifting forces were only achieved at low lifting speeds. Another limitation is that only one plug was formed in the test setup. It would be valuable to investigate the influence of multiple plugs on the conveying resistance in future research.

Funding

The work was supported by the Shanghai Science and Technology Plan [grant number 22dz1204102]; Shanghai Pujiang Project [grant number 21PJ1404600]; and International Association of Maritime Universities [grant number 20220304].

CRedit authorship contribution statement

Xiangwei Liu: Writing – review & editing, Writing – original draft, Methodology, Funding acquisition, Conceptualization. **Shuhao Yang:** Methodology, Investigation, Formal analysis, Data curation. **Yusong Pang:** Writing – review & editing, Supervision, Formal analysis, Conceptualization.

Declaration of competing interest

The authors declare that they have no known competing financial interests or personal relationships that could have appeared to influence the work reported in this paper.

Data availability

Data will be made available on request.

Acknowledgements

The authors would like to express their deep appreciation to Prof. Haim Kalman from Ben-Gurion University of the Negev, and Prof. Andre Katterfeld from University of Magdeburg for their inspiring discussions during this study.

References

- Alhaddad, S., Mehta, D., Helmons, R., 2023. Mining of deep-seabed nodules using a Coandă-Effect-based collector. *Results Eng.* 17, 100852.
- Bartosik, A., 2020. Validation of friction factor predictions in vertical slurry flows with coarse particles. *J. Hydrol. Hydromech.* 68, 119–127.
- Bear, J., 1972. *Dynamics of Fluids in Porous Media*. Elsevier, New York.
- Chung, J., Yarim, G., Savasci, H., 1998. Shape effect of solids on pressure drop in a 2-phase vertically upward transport: silica sands and spherical beads the Eighth International Offshore. *Polar Engineering Conference. ISOPE*, Montreal, Canada.
- Coker, A.K., 2007. Fluid flow. In: *Ludwig's Applied Process Design for Chemical and Petrochemical Plants*. Elsevier, pp. 133–302. <https://doi.org/10.1016/B978-075067766-0/50011-7>.
- Durand, R., 1953. Basic relationships of the transportation of solids in pipes – experimental research. In: *Proceedings of the Minnesota International Hydraulics Convention*, pp. 89–103.
- Engelmann, H., 1978. Vertical hydraulic lifting of large-size particles a contribution to marine mining. In: *Proceedings of the 10th Offshore Technology Conference*, pp. 731–740.
- Ergun, S., 1952. Fluid flow through packed columns. *Chem. Eng. Prog.* 48, 89.
- Feng, Z.G., Michaelides, E.E., 2003. Equilibrium position for a particle in a horizontal shear flow. *Int. J. Multiphase Flow* 29, 943–957. [https://doi.org/10.1016/S0301-9322\(03\)00061-2](https://doi.org/10.1016/S0301-9322(03)00061-2).
- Hein, J.R., Mizell, K., Koschinsky, A., Conrad, T.A., 2013. Deep-ocean mineral deposits as a source of critical metals for high- and green-technology applications: comparison with land-based resources. *Ore Geol. Rev.* 51, 1–14. <https://doi.org/10.1016/j.oregeorev.2012.12.001>.
- Kang, Y., Liu, S., 2021. The development history and latest progress of deep-sea polymetallic nodule mining technology. *Minerals* 11, 1132. <https://doi.org/10.3390/min11101132>.
- Konrad, K., 1980. Prediction of the pressure drop for horizontal dense phase pneumatic conveying of particles. In: *Proceedings of the 5th International Conference on Pneumatic Transport of Solids in Pipes*, pp. 225–244.
- Konrad, K., Totah, T.S., 1989. Vertical pneumatic conveying of particle plugs. *Can. J. Chem. Eng.* 67, 245–252.
- Lee, C., Hong, S., Kim, H., Kim, S., 2015. A comparative study on effective dynamic modeling methods for flexible pipe. *J. Mech. Sci. Technol.* 29 (7), 2721–2727.
- Li, M., He, Y., Liu, Y., Huang, C., 2018. Pressure drop model of high-concentration graded particle transport in pipelines. *Ocean Eng* 163, 630–640. <https://doi.org/10.1016/j.oceaneng.2018.06.019>.
- Li, M., He, Y., Liu, W., Liu, Y., Huang, C., Jiang, R., 2020. Effect of adding finer particles on the transport characteristics of coarse-particle slurries in pipelines. *Ocean Eng* 218, 108160. <https://doi.org/10.1016/j.oceaneng.2020.108160>.
- Liu, X., Yang, S., 2024. Prediction of conveying resistance for a novel hydraulic-mechanical hybrid vertical lifting system. *Mod Subsea Eng Technol* 2, 2. <https://doi.org/10.53964/mset.2024002>.
- Ma, W., Zhang, K., Du, Y., Liu, X., Shen, Y., 2022. Status of sustainability development of deep-sea mining activities. *J. Mar. Sci. Eng.* 10, 1508. <https://doi.org/10.3390/jmse10101508>.
- Matousek, V., 2009. Pipe-wall friction in vertical sand-slurry flows. *Part. Sci. Technol.* 27, 456–468. <https://doi.org/10.1080/02726350903133179>.
- Messa, G.V., Malavasi, S., 2013. Numerical investigation of solid-liquid slurry flow through an upward-facing step. *J. Hydrol. Hydromech.* 61, 126–133. <https://doi.org/10.2478/johh-2013-0017>.
- Miedema, S., 2017. *Slurry Transport: Fundamentals, Historical Overview & the Delft Head Loss & Limit Deposit Velocity Framework*. <https://doi.org/10.5074/t.2019.002>.
- Newitt, D., 1955. Hydraulic conveying of solids in horizontal pipes. *Chem. Engrs. Instr.* (Trans.) 33, 93–110.
- Niederreiter, G., Sommer, K., 2004. Modeling and experimental validation of pressure drop for pneumatic plug conveying. *Granul. Matter* 6, 179–183. <https://doi.org/10.1007/s10035-004-0171-0>.
- Rabinovich, E., Freund, N., Kalman, H., Klinzing, G., 2012. Friction forces on plugs of coarse particles moving upwards in a vertical column. *Powder Technol.* 219, 143–150. <https://doi.org/10.1016/j.powtec.2011.12.030>.
- Sharma, R., 2022. *Perspectives on Deep-sea mining: sustainability, technology, Environmental Policy, and Management*. Springer, Nature Switzerland AG, Cham, Switzerland.
- Shaul, S., Kalman, H., 2014. Friction forces of particulate plugs moving in vertical and horizontal pipes. *Powder Technol.* 256, 310–323. <https://doi.org/10.1016/j.powtec.2014.02.036>.
- Shook, C.A., Bartosik, A.S., 1994. Particle–wall stresses in vertical slurry flows. *Powder Technol.* 81, 117–124.
- Sperl, M., 2006. Experiments on corn pressure in silo cells – translation and comment of Janssen's paper from 1895. *Granul. Matter* 8, 59–65. <https://doi.org/10.1007/s10035-005-0224-z>.
- van Wijk, J.M., van Rhee, C., Talmon, A.M., 2014. Wall friction of coarse grained sediment plugs transported in a water flow through a vertical pipe. *Ocean Eng* 79, 50–57. <https://doi.org/10.1016/j.oceaneng.2014.01.010>.
- van Wijk, J.M., De Hoog, E., Talmon, A.M., Van Rhee, C., 2022. Concentration and pressure measurements of dense sand and gravel multiphase flows under transient flow conditions in a vertically oriented closed conduit – assessment of system and sensor performance. *Flow Meas. Instrum.* 84, 102126 <https://doi.org/10.1016/j.flowmeasinst.2022.102126>.
- Wasp, E.J., Kenny, J.P., Gandhi, R.L., 1977. *Solid-liquid flow: slurry pipeline transportation, Ser. Bulk Mater* 1, 224.
- Wilson, K., 1965. *Application of the Minimum Entropy Production Principle to Problems in Two-phase Flow*. Queen's University, Kingston, Ontario, Canada.
- Wu, J., Yu, B., Yun, M., 2008. A resistance model for flow through porous media. *Transp. Porous Med.* 71, 331–343.
- Wu, Y., Sima, C., Zhu, Z., 2022. Key development directions of marine science and technology. *Sci Technol Foresight* 1, 20–35.
- Xia, J., 2002. Pressure loss in solid-liquid flow with coarse manganese nodules in vertical pipeline. *J. Sediment. Res.* 2, 23–27.
- Yang, Y., Zhang, P., He, L., Sun, J., Huang, Z., Wang, J., Yang, Y., 2020. Acoustic analysis of particle-wall interactions of plug flow in vertical pneumatic conveying. *Chem. Eng. Sci.* 211, 115260 <https://doi.org/10.1016/j.ces.2019.115260>.
- Yokojima, S., Takashima, R., Asada, H., Miyahara, T., 2021. Impacts of particle shape on sedimentation of particles. *Eur. J. Mech. B Fluids* 89, 323–331. <https://doi.org/10.1016/j.euromechflu.2021.06.007>.
- Yu, B., Li, J., 2004. A geometry model for tortuosity of flow path in porous media. *Chin. Phys. Lett.* 21, 1569–1571. <https://doi.org/10.1088/0256-307X/21/8/044>.